

Weak ferromagnetism in cobalt oxalate crystals

E Romero¹, M E Mendoza¹ and R Escudero²

¹*Instituto de Física, Universidad Autónoma de Puebla,
Apartado Postal J-48, Puebla 72570, México and*

²*Instituto de Investigaciones en Materiales, Universidad Nacional Autónoma de México,
Apartado Postal 70-360, México DF 04510, México**

(Dated: August 14, 2018)

Microcrystals of diaquocobalt(II) oxalate have been synthesized by the coprecipitation reaction of aqueous solutions of Cobalt (II) bromide and oxalic acid. Chemical analysis and thermal experiments revealed that there is only one phase present. X-ray powder diffraction studies show that this compound is orthorhombic with space group $Ccmm$. Molar susceptibility versus temperature measurements show the existence of an antiferromagnetic ordering, however, the hysteresis measured in magnetization measurements as a function of magnetic field reveals a weak ferromagnetic behavior.

PACS numbers: 75.30.Fv; 75.50.Xx; 75.75.Cd

I. INTRODUCTION

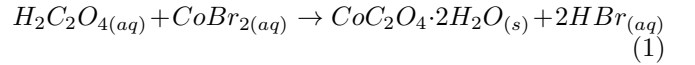
Oxalates dihydrates containing divalent 3d transition elements, with general formula $MC_2O_4 \cdot nH_2O$ where M is a metallic ion 2+ [1–11], exhibit quasi-one-dimensional magnetic behavior characterized by a dominant magnetic correlation along oxalate-metal ion chains. Kurmoo [12] has reported a weak antiferromagnetic interaction in these compounds. However, it is expected that in systems like the aforementioned oxalates, with many close chains [13], the intra- and inter-chains magnetic interactions cant the spins, distorting the antiferromagnetic order and producing also a weak ferromagnetism (WF). At low temperatures the WF behavior will be presumably more pronounced.

Cobalt oxalate dihydrate is a quasi-one dimensional magnetic compound useful to search the existence of WF at low temperature because, it crystallizes in two allotropic forms [14]: α – *monoclinic*, space group $C2/c$, $a = 11.775 \text{ \AA}$, $b = 5.416 \text{ \AA}$, $c = 9.859 \text{ \AA}$ and $\beta = 127.9^\circ$, and β – *orthorhombic*, $Ccmm$, $a = 11.877 \text{ \AA}$, $b = 5.419 \text{ \AA}$, and $c = 15.624 \text{ \AA}$. Both structures are formed by identical infinite chains of $[CoC_2O_4 \cdot 2H_2O]$ units, the difference between them lies in the relative displacement of adjacent chains along b -axis [15–18]. Each Co^{2+} ion is surrounded by distorted oxygen octahedron, where four oxygens belong to the oxalate anions and the other two to the water molecules. The more stable α structure is the most studied. Its magnetic structure [19], has been described as two interpenetrating antiferromagnetic sublattices belonging to the Shubnikov group P_6c , with parameters a , $2b$, c . There was found that below the Néel temperature $T_N = 6.1 \text{ K}$, three-dimensional antiferromagnetic long-range order exists, corresponding to a collinear magnetic structure with $k = [0, 1/2, 0]$ and magnetic moments aligned parallel to the a axis.

In this paper, we will report results on the synthesis, crystal structure, and magnetic measurement of the orthorhombic $\beta - CoC_2O_4 \cdot 2H_2O$ microcrystals. It was determined by M-H measurements from 2 - 200 K, that this phase exhibits WF ordering at $T < 7.5 \text{ K}$.

II. EXPERIMENTAL METHODS

The synthesis of orthorhombic β – cobalt oxalate dihydrate was carried out by coprecipitation reaction of aqueous solutions of cobalt (II) bromide 0.1 M (Aldrich, 99%) and oxalic acid 0.00625 M (Aldrich, $\geq 99\%$), according to the chemical equation,



The precipitates were filtered and dried at room temperature.

Morphological analyses were performed with a scanning electron microscope (SEM) Cambrige-Leica Stereoscan 440. Powder X-ray diffraction patterns were acquired using a Siemens D5000 diffractometer, operating in the Bragg-Brentano geometry with $\lambda(Cu-K\alpha) = 1.541 \text{ \AA}$, and 2θ scan = 10 - 70°, with a step size of 0.02°. Thermogravimetric (TG) and differential thermal analysis (DTA) curves were obtained in a SDT-TA Instruments model 2960, in air atmosphere with heating rate of 5 °C/min from room temperature up to 600 °C. Heat capacity was measured between 2 and 300 K in a Quantum Design PPMS system. Magnetization measurements were performed in a Quantum Design MPMS SQUID magnetometer, MPMS-5. Zero Field Cooling (ZFC) and Field Cooling (FC) cycles were performed at magnetic intensities of 1T, in the range from 2 to 300 K. Isothermal magnetization measurements $M(H)$ were obtained at 2, 50, 100, 160 and 200 K. The diamagnetic contribution calculated from Pascal's constants [20] was $\chi_{Di} = -72 \cdot 10^{-6} \text{ cm}^3/\text{mol}$.

*Author to whom correspondence should be addressed. RE, email address:eromero@sirio.ifuap.buap.mx

III. RESULTS AND DISCUSSION

A. Synthesis and Morphology

Five polycrystalline samples were obtained using different reaction times (see Table I). Pink cobalt oxalate dihydrate microcrystals were obtained after dry precipitates at room temperature. Chemical analysis by digestion using Inductively Coupled Plasma-Optical Emission Spectrometry (ICP-OEP), by combustion using Thermal Conductivity-Infrared (TCD/IR), and Pyrolysis-IR, give the composition in weight of 35 % in cobalt, 13.21 % in carbon, 2.45 % in hydrogen, and 54.92 % in oxygen. The morphology shown by all the precipitates is tubular-like (inset in Fig. 1), generated by self-assembly of needle-like microcrystals as shown in Fig. 1.

The observed microtubes have an average length size (L) and a diameter (D) in the range from 16 - 146.2 and 0.6 - 3.8 μm respectively. This morphology is not the usual one for the cobalt oxalates prepared by precipitation methods from homogeneous solutions without additives.

Some reports concerning to the morphology of 3d ions oxalates prepared by precipitation reactions have been published, Pujol et al. [21] have found that cobalt oxalate dihydrate crystals present a rod-like morphology. They used as reactant solutions cobalt nitrate and sodium oxalate. Jongen et al. [22] have also obtained copper oxalate with controlled morphology from cushion to rod-like crystals, using solutions of copper nitrate and sodium oxalate, adding a polymer at different concentrations. These authors show that the mechanism of growth is by self-assembly, guided by the copper oxalate crystal structure. Additionally, nanorods of nickel oxalate were synthesized using solutions of nickel nitrate and ammonium oxalate adding a cationic surfactant (CTAB) [23]. Negative surface charge on the nanorods was observed, it has a bearing on the growth of the rods along the cross-section, especially with surfactant molecules having positively charged headgroups (CTAB).

It is known that in crystal growth in aqueous solutions, there is a correlation between the ionic strength of the solution and the kinetics of crystal faces [24]. In order to explain the morphology of our orthorhombic β - $\text{CoC}_2\text{O}_4 \cdot 2\text{H}_2\text{O}$ crystals obtained in this work, and compared with the reported by Pujol, we calculated the ionic strength of the solutions in both cases using the Debye equation $I = 1/2 \sum C_i Z_i^2$, where I is the ionic strength, C_i and Z_i are the concentration and charge of ions i , respectively [25]. Whereas Pujol et al. [21] used cobalt nitrate 0.0052 M and sodium oxalate 0.005 M, in our work we used cobalt bromine 0.00625 M, and oxalic acid 0.1 M. The calculated ionic strength were 0.0306 M [21] and 0.3187 M, (this work) with a difference between them about one order of magnitude.

Additionally, in our work the pH at the end of reaction was 1.5, then this high concentration of H^+ ions would assembly on the negative surface of the cobalt oxalate

crystals growing, and the high ionic strength of the solutions screening the self-assembly of crystallites, giving as a final result the tubular-like morphologies.

Sample	TG	D(μm)	L(μm)
S1	12 min	0.6	16.0
S2	12 h	1.4	53.3
S3	24 h	1.5	55.4
S4	40 h	2.1	79.9
S5	7 days	3.8	146.2

TABLE I: Polycrystalline samples obtained using different reaction times. TG denotes growth time, D and L are average diameter and length of the particles, respectively.

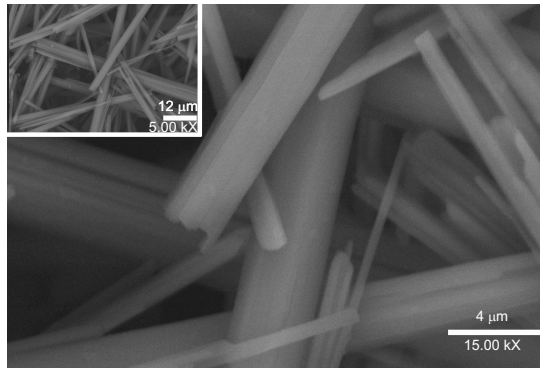


FIG. 1: (Color online) SEM micrograph of cobalt oxalate needles-like crystallites forming tubular microcrystals, for sample S4.

B. Diffraction pattern

Monoclinic α phase of $\text{CoC}_2\text{O}_4 \cdot 2\text{H}_2\text{O}$ is characterized by the presence of a doublet peak in the XRD powder diagram, it is at $2\theta = 18.745^\circ$ [18].

Fig. 2a displays the XRD powder diffraction pattern of the sample S4 (blue pattern); in good agreement with the reported pattern (red lines) for the orthorhombic β -phase of cobalt oxalate dihydrate (JCPDS file: 25-0250). In all other samples (S1, S2, S3 and S5) the same phase was identified.

Rietveld refinement [26] of the pattern was performed using the Win-Rietveld software, the background was estimated by linear interpolation, and the peak shape was modeled by a Pseudo-Voigt function. Unit cell parameters used were $a = 11.877\text{\AA}$, $b = 5.419\text{\AA}$, and $c = 15.624\text{\AA}$ [14]. The atomic positions were the reported by Deyrieux et al. for iron-oxalate [17]: $4\text{Co}(\frac{1}{4}, \frac{1}{4}, 0)$, $4\text{Co}(0, 0, \frac{1}{4})$, $8\text{C}_{oxalate}(\frac{1}{4}, \frac{3}{4}, 0.041)$, $8\text{C}_{oxalate}(0, \frac{1}{2}, 0.291)$, $16\text{O}_{oxalate}(\frac{1}{4}, 0.941, 0.089)$, $16\text{O}_{oxalate}(0, 0.691, 0.339)$, $8\text{O}_{water}(0.419, \frac{1}{4}, 0)$, $8\text{O}_{water}(0.169, 0, \frac{1}{4})$. The weighted profile and expected residual factors obtained by the Rietveld

refinement were $R_{wp} = 20.04$ and $R_{exp} = 9.95$. The refined cell parameters determined for the Co-oxalate orthorhombic phase in all samples were $a = 11.879(4)$ Å, $b = 5.421(2)$ Å, and $c = 15.615(6)$ Å. A schematic representation of the unit cell is shown in Fig. 3. In this figure there are two non-equivalent positions for the cobalt ions, designed as Co1 and Co2, each cobalt ion is shifted respect to other by a translation vector $(\frac{1}{2}, \frac{1}{2}, 0)$.

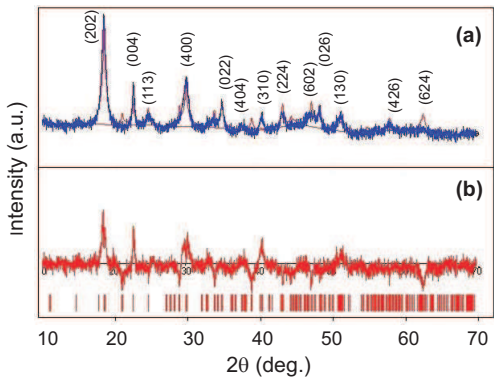


FIG. 2: (Color online) (a) X-Ray powder diffraction data of sample $S4$ (blue pattern), Miller indices for orthorhombic $Cccm$ (JCPDS file: 25-0250). The theoretic structural (red pattern) was performed using the Win-Rietveld software. (b) Refinement difference.

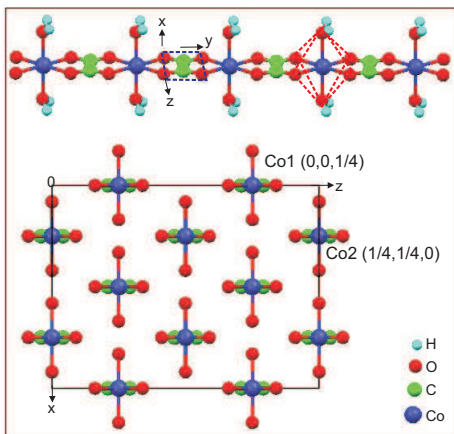


FIG. 3: (Color online) Co-oxalate unit cell of the orthorhombic β -phase of JCPDS file 25-0250, space group $Cccm$. There are eight cobalt atoms located in two non-equivalent positions designed as Co1 and Co2.

Finally, mean crystallite dimension (D) for the sample was calculated with the Scherrer equation (Eq. 2) using the (202) peak.

$$D = \frac{0.9\lambda}{(B - b)\cos\theta}, \quad (2)$$

where λ is the wavelength of the radiation, B is the width of the diffraction line at half intensity maximum, and b

is the instrumental broadening, 0.05 , θ is the diffraction angle. The calculated values were 21.4 nm for $S1$, $S2$, and $S3$ samples, 22.7 nm for $S4$, and 26.4 nm for $S5$ sample.

C. Thermal analysis

TG studies of all samples of $CoC_2O_4 \cdot 2H_2O$ have shown two steps of weight loss, the first one occurring at about 150 °C, and the second one at about 270 °C. Fig. 4 presents the TG curve for sample $S4$. In the first step the weight loss of 18.5% corresponds to two water molecules, this is according to the theoretical value of 19.7% . The DTA curve associated with this process shows an endothermic peak at about 145 °C. The dehydration reaction is



The weight loss of 36.4% in the second step may be attributed to the decomposition of the anhydrous cobalt oxalate to obtain cobalt oxide. This agrees with the theoretical value [27]. The corresponding DTA curve shows an exothermic peak, about $T = 267$ °C. The decomposition reaction in this step can be written as:

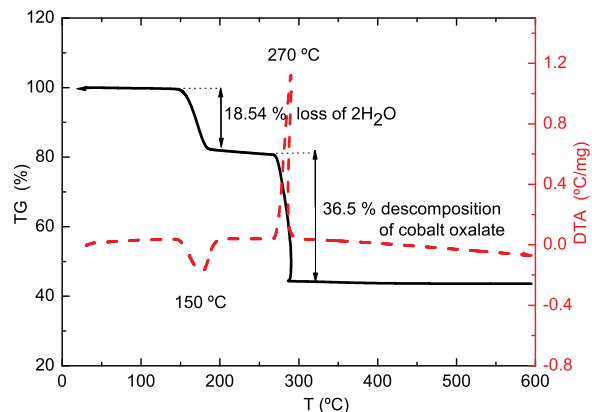
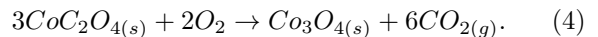


FIG. 4: (Color online) TG(solid line)/DTA(dash line) curves for $CoC_2O_4 \cdot 2H_2O$ (sample $S4$) at 5 °C/min heating rate.

It is important to observe that the absence of any additional peak on TG and DTA curves, indicates the high purity of the cobalt oxalate samples.

D. Heat capacity

Heat capacity of $\beta - CoC_2O_4 \cdot 2H_2O$ (sample $S4$) is plotted as function of temperature in Fig. 5. The most

important feature is the sharp λ -peak occurring at about 7.5 K. It is important to mention that for $\alpha - CoC_2O_4 \cdot 2H_2O$, the λ -peak was reported at about $T = 6.23$ K, indicating the onset of long-range magnetic order [28] and consistent with the Néel temperature $T_N = 6.1 + 0.1$ K found in deuterated cobalt oxalate [19]. So for $\beta - CoC_2O_4 \cdot 2H_2O$ we report a Néel temperature at about 7.5 K.

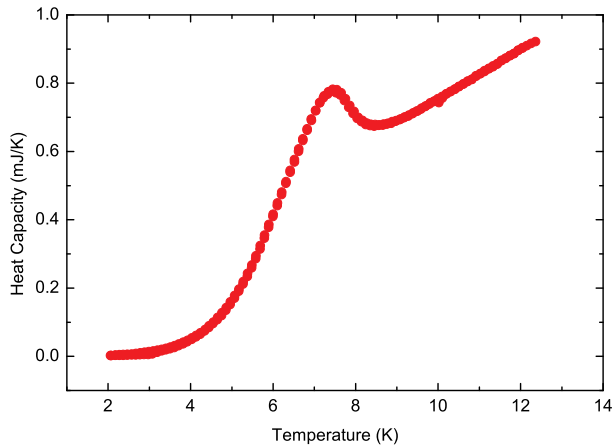


FIG. 5: (Color online) Heat capacity of $\beta - CoC_2O_4 \cdot 2H_2O$, sample S4. Peak at $T = 7.5$ K. This lambda peak represents the AF transition with onset at about 8.2 K, maximum at 7.5 K.

E. Magnetic measurements

The molar susceptibility - Temperature ($\chi(T)$), for the five samples (S1-S5) is shown in Fig. 6. It was measured at magnetic field of 1T in both ZFC, and FC modes. All samples have almost the same behavior, at low temperature the magnetic susceptibility values are small, it increases rapidly as the temperature increases up to a maximum close to 24 K, see inset of Fig. 6. As the temperature is raised $\chi(T)$ smoothly decreases up to a minimum at room temperature. Although χ_{max} values are different in all samples (varying in the range of 3.3×10^{-2} to $4.08 \times 10^{-2} \text{ cm}^3/\text{mol}$), they are similar to those reported for $\alpha - CoC_2O_4 \cdot 2H_2O$ where $\chi_{max} = 3.6 \times 10^{-2} \text{ cm}^3/\text{mol}$ [28]. From room temperature to 100 K a Curie-Weiss behavior clearly can be fitted.

The maximum on susceptibility at $T_{max} = 24$ K, is a typical behavior of the susceptibility occurring in low dimensional antiferromagnets [12, 29], this curve is correctly predicted by

$$\frac{\chi_{max}|J|}{g^2\mu_B^2} = 0.07346, \quad (5)$$

at

$$\frac{k_B T_{max}}{|J|} = 1.282, \quad (6)$$

with $g = 2$ (for 3d ions), $\mu_B = 9.27 \times 10^{-24}$ and $k_B = 1.38 \times 10^{-23}$, it was obtained a value $|J| / k_B = 18.72$ K, i.e. $|J| = 1.6$ meV.

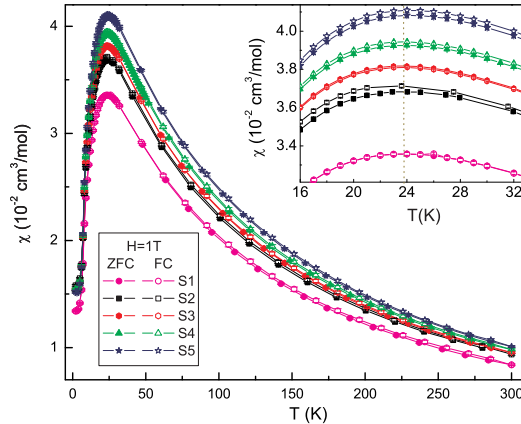


FIG. 6: (Color online) Molar susceptibility ($\chi(T)$) of 5 samples of $\beta - CoC_2O_4 \cdot 2H_2O$, with maximum at 24 K, measured for ZFC and FC modes, with $H = 1$ T. Full colors (solid symbols) represent ZFC measurements, whereas open symbols is FC mode.

In the case of nickel oxalate chains, Keene et al. [6] have modeled the behavior of an antiferromagnetically coupled chain of quantum spins by a polynomial approximation (Eq. 7).

$$\chi_{cal} = \frac{N\mu_B^2 g^2}{k_B T} \left[\frac{A + Bx^2}{C + Dx + Ex^3} \right], \quad (7)$$

where $x = |J| / k_B T$. Using this model for the molar susceptibility of β -cobalt oxalate χ_{exp} (solid line), in Fig. 7 a good fit (dash line) is obtained with $|J| / k_B = 18.72$ K, T (2 K - 300 K), $g = 2.51$, $A = 1.3667$, $B = 1.36558$, $C = 1$, $D = 2.3018$ and $E = 5.7448$.

The maximum shown in the susceptibility in figures 6 and 7 is a characteristic feature of the effect of spins fluctuations as described by the Heisenberg model [5]. The inset of Fig. 6 shows the molar susceptibility versus temperature from 16 to 32 K. Here, FC and ZFC modes present a small irreversibility that gives a hysteretic behavior at about 30 K with the maximum at about 24 K. This irreversibility corroborates the spin fluctuating characteristics at this temperature. At high temperatures the system tends clearly to be in a paramagnetic state. When the temperature decreases thermal energy will be small and spin fluctuations tend to be canceled and aligned in a minimum energy configuration.

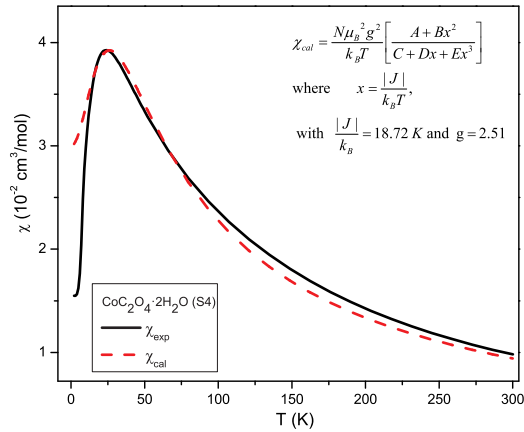


FIG. 7: (Color online) Molar susceptibility ($\chi_{exp}(T)$, solid line) of $\beta - CoC_2O_4 \cdot 2H_2O$ (sample $S4$) and the fit ($\chi_{cal}(T)$, dash line) for antiferromagnetically coupled chain of quantum spins.

Our results are similar to those reported for oxalate-cobalt (II) complexes [7, 30, 31]. However our experimental observations show that this broad maximum may be due to the competition of two different magnetic ordering, an uncompensated antiferromagnetism, and consequently a weak ferromagnetism.

In Fig. 8 it is show a plot of the inverse of susceptibility, χ^{-1} as a function of temperature at $H = 1T$, for all samples.

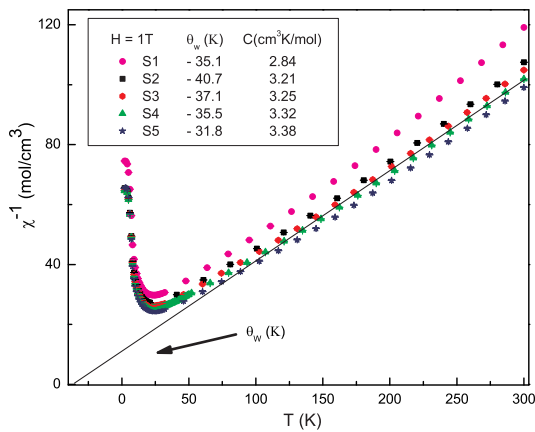


FIG. 8: (Color online) Inverse susceptibility $\chi^{-1}(T)$ corresponding to 5 samples. Weiss temperature θ_w , changes from -35.8 to -40.7 K. Curie constant also changes from 2.84 to 3.38 $cm^3 mol^{-1}K$.

The analysis of these measurements was performed by fitting a Curie-Weiss behavior above 100 K, where the fit parameters; Weiss temperature θ_w , and Curie constant C, varying from -31.8 to -40.7 K and from 2.84 to 3.38 $cm^3 mol^{-1}$, respectively.

These data permit calculate the effective magnetic moment μ_{eff} per mole, according to the equation $\mu_{eff} = 2.84[C]^{1/2} = 2.84[\chi(T - \theta_w)]^{1/2}$. In Fig. 9, the effective number of Bohr magnetons at room temperature for each sample ($S1 - S4$) is different (4.76, 5.07, 5.09, 5.15, 5.19 μ_B). However, it is in agreement with reported values in studies of layered transition metal oxalates [32] where for octahedrally coordinated cobalt(II) with a $^4T_{1g}$ ground term the observed moment is typically 4.7 - 5.2 μ_B . After calculation of μ_{eff} , the number of unpaired electrons n in $\beta - CoC_2O_4 \cdot 2H_2O$, using $\mu_{eff} = g[n(n+1)]^{1/2}$ can be calculated. Those values for each sample are in the range of 1.94 to 2.15.

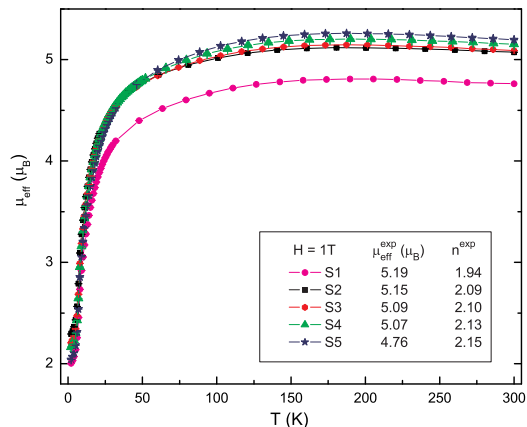


FIG. 9: (Color online) Effective Bohr magnetons, μ_{eff} per mole as a function of temperature. At room temperature the values are between 4.76 to 5.15 μ_B . n is the number of unpaired electrons.

The decrease in $\mu_{eff}(T)$ on cooling and the large negative Weiss temperature, indicate an antiferromagnetic coupling between neighboring ions, for all samples ($S1 - S5$).

It is important to mention that short-range order is observed in materials with a low-dimensional magnetic character, where strong magnetic interactions between the nearest ions are along the chains [32]. To understand more about the magnetic characteristics of this oxalate, we studied the M-H isothermal measurements in the temperature range from 2 - 200 K, the resulting data is shown in Fig. 10 for the sample $S4$.

As can be noted in the inset of Fig. 10, the magnetization never reaches a saturation value, the M-H curve behaves almost in linear form, thus characteristic of an

AF order. However, a careful observation at low fields, show a small, but measurable hysteretic behavior.

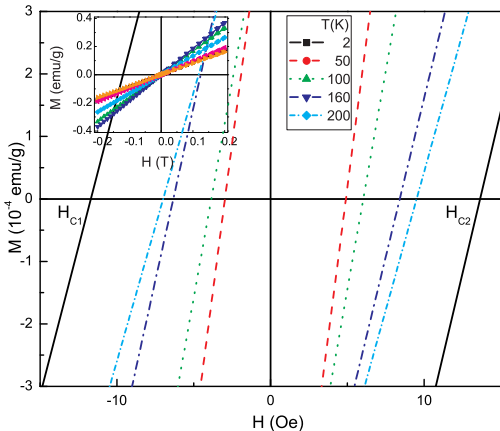


FIG. 10: (Color online) Isothermal magnetization measurements M - H from 2 to 200 K shown in the main panel. Inset shows the magnetization at high field and different temperatures from 2 to 200 K. At low fields (main panel) the hysteretic effect is clearly observed. The asymmetric behavior in the coercive field might be related to a exchange bias effect due to an uncompensated or canted antiferromagnetism, but other type of interaction are not discarded as driven by Dzyaloshinsky-Moriya type exchange (DM).

In order to clarify the existence of the hysteretic effect, studies of the coercive field H_C as a function of temperature were performed. Fig. 11, shows H_C versus T for sample $S4$. Here we see the evidence of the asymmetric behavior related of the coercive field, thus implying an exchange bias effect $H_{C1} \neq H_{C2}$ due to two competing magnetic ordering: AF and a WF. All studied samples have similar behavior. This exchange bias can be explained as the effect of inter and intra chains interaction in this compound. The effect of interaction of metallic ions between chains is canting the spins. This small but measurable exchange bias indicates that in place to have a pure antiferromagnetic order the magnetic order will be distorted by uncompensated antiferromagnetism due to canted spins. Thus two magnetic orders will be the result: a canted antiferromagnetism, and a weak ferromagnetism. In this study all our studied samples presented similar behavior. It is important to mention that great care was taken when measuring the exchange bias. Our SQUID magnetometer is provided with a Mu metal shielding. At the moment of performing the magnetization measurements a flux gate magnetometer was used to demagnetize the superconducting coil. This procedure reduces the magnetic field to a very small value to about 0.001 G, or less and the Mu shielding eliminates external magnetic influences, as the earth magnetic field.

In figure 11 we observe that at 2 K the coercive field

is about +13 Oe and -13 Oe and decreases rapidly to a minimum value of 3 Oe, at temperatures close to 20 K. Above 20 K the coercive field increases in a smooth form reaching a value of 8 Oe at room temperature. This small but measurable coercive field clearly indicates a system with canted spins, thus a competition between possible DM interaction antiferromagnetism and weak ferromagnetism.

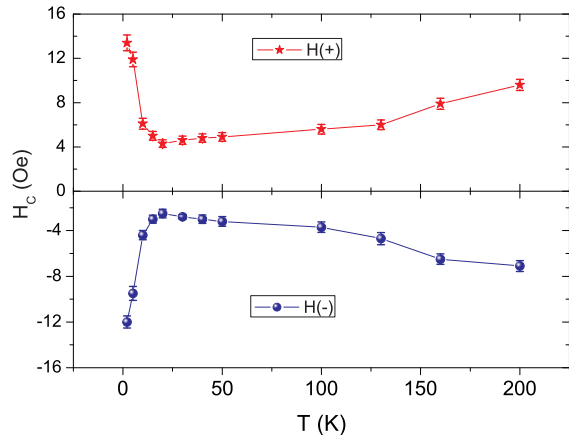


FIG. 11: (Color online) Coercive Field vs Temperature as determined by isothermal magnetic measurements for sample $S4$. Note the minimum at about 20 K.

Evidently the situation at low temperatures is more complicated. Analysis of the susceptibility data for cobalt(II) complexes may show deviation from simple Curie-Weiss behavior [31] by different mechanism: single-ion, orbital moments, spin-orbit coupling, distortions from regular stereochemistry and crystal field and also DM interactions. All these processes clearly may affect the magnetic properties.

The ground state of the free Co(II) ion is 4F , but the orbital degeneracy is removed in an octahedral crystal field giving a $^4T_{1g}$ ground state. The combined effect of the spin-orbit coupling and the axial or rhombic distortions of the crystal field most often gives rise to six Kramers doublets, two are much lower in energy. When the temperature is low enough, only the ground Kramers doublet is thermally populated and the Co(II) ion can be formally treated with an effective spin $S = 1/2$ and a very anisotropic g tensor [28]. In the case of $\beta\text{-CoC}_2\text{O}_4 \cdot 2\text{H}_2\text{O}$ this temperature is low enough and is close to 7.5 K.

Reports on magnetic studies of some chain and layered six-coordinated cobalt(II) compound [6, 31] show that, at low temperature, these magnetic systems behave as a collection of Ising chain with $S = 1/2$ effective spin coupled ferromagnetically, and/or with antiferromagnetically interactions [31]. It is necessary to note that the Ising model is restricted to the temperature range where

only the ground Kramers doublet are thermally populated, thus ($T < 40$ K). However, at high temperatures a crossover to the Heisenberg type behavior is expected.

IV. CONCLUSIONS

Microcrystals of cobalt (II) oxalate were prepared by soft solution chemistry. XRD powder diffraction patterns show a orthorhombic phase. Chemical analysis, DTA and TG studies revealed that the microcrystals have high purity. χ -T measurements reveal the existence of an AF ordering, by interaction of coupled chains via inter and intra interactions, and/or DM type-exchange. Those ef-

fects of interchain interaction affects the AF coupling, distorting it and canting spins producing a weak ferromagnetism ordering. This WF and canted AF is evident by hysteresis measurements in M-H studies.

Acknowledgments

Partial support for this work is gratefully acknowledge to CONACyT, project No.44296/A-1 and Scholarship CONACyT, register No. 188436 for E. Romero; VIEP-BUAP, project No. MEAM-EXC10-G. We also thank F. Morales for providing the Heat Capacity measurements.

-
- [1] S. Decurtins, M. Verdaguer, *Phil. Trans. R. Soc. Lond. A* **357**, 3025 (1999)
- [2] J. S. Miller and A. J. Epstein, *MRS Bull.* **25**, 21 (2000).
- [3] V. I. Ovcharenko, R. Z. Sagdeev, *Russ. Chem. Rev.* **68**, 345 (1999).
- [4] A. R. West, *Solid State Chemistry and its Applications* (John Wiley & Sons, New York, 1984), p. 553.
- [5] S. J. Blundell and F. L. Pratt, *J. Phys.: Condens. Matter* **16**, R771 (2004).
- [6] S. Simizu, J. Y. Chen, S. A. Friedberg, J. Martinez and G. Shirane, *J. Appl. Phys.* **61**, 3420 (1987).
- [7] N. S. Ovanesyan, G. V. Shilov, A. A. Pyalling, C. Train, P. Gredin, M. Gruselle, L. F. Kiss and L. Botton, *J. Magn. Magn. Mater.* **272**, 1089 (2004).
- [8] K. Awaga, E. Coronado and M. Drillon, *MRS Bull.* **25**, 52 (2000).
- [9] M. B. Hursthouse, M. E. Light and D. J. Price, *Angew. Chem. Int. Ed.* **43**, 472 (2004).
- [10] T. D. Keene, H. R. Ogilvie, M. B. Hursthouse and D. J. Price, *Eur. J. Inorg. Chem.*, 1007 (2004).
- [11] D. J. Price, A. K. Powell and P. T. Wood, *J. Chem. Soc., Dalton Trans.*, 3566 (2000).
- [12] M. Kurmoo, *Chem. Soc. Rev.* **38**, 1353 (2009).
- [13] J. Bacsá, D. Eve and K. R. Dunbar, *Acta Cryst.* **C61**, m58 (2005).
- [14] R. Deyrieux, C. Berro and A. Pélououx, *Bull. Soc. Chim. Fr.* **1**, 25 (1973).
- [15] P. J. Dubernat and H. Pezerat, *J. Appl. Cryst.* **7**, 378 (1974).
- [16] M. Molinier, D. J. Price, P. T. Wood and A. K. Powell, *J. Chem. Soc., Dalton Trans.*, 4061 (1997).
- [17] R. Deyrieux and A. Pélououx, *Bull. Soc. Chim. Fr.*, 2675 (1969).
- [18] C. Drouet, A. Pierre and A. Rousset, *Solid State Ionics* **123**, 25 (1999).
- [19] I. Sledzinska, A. Murasik and P. Fisher, *J. Phys. C: Solid State Phys.* **21**, 5273 (1988).
- [20] G. A. Bain and J. F. Berry, *J. Chem. Educ.* **85**, 532 (2008).
- [21] O. Pujol, P. Bowen, P. A. Stadelmann and H. Hofmann, *J. Phys. Chem. B* **108**, 13128 (2004).
- [22] N. Jongen, P. Bowen, J. Lemaitre, J. C. Valmalette and H. Hofmann, *J. Colloid Interf. Sci.* **226**, 189 (2000).
- [23] S. Vaidya, P. Rastogi, S. Agarwal, S. K. Gupta, T. Ahmad, A. M. Antonelli, K. V. Ramanujachary, S. E. Lofland and K. Ganguli, *J. Phys. Chem. C* **112**, 12610 (2008).
- [24] T. Sugimoto and E. Matijevic, *J. Coll. Int. Sci.* **74**, 227 (1980).
- [25] G. H. Ayres, *Anlisis Quimico Cuantitativo* (Ed. Harla, México, 1970), p. 59.
- [26] L. B. McCusker, R. B. Von Dreele, D. E. Cox, D. Louër and P. Scardi, *J. Appl. Cryst.* **32**, 36 (1999).
- [27] W.-W. Wang and Y.-J. Zhu, *Mater. Res. Bull.* **40**, 1929 (2005).
- [28] J. A. Lukin, S. Simizu, N. S. VanderVen and S. A. Friedberg, *J. Magn. Magn. Mater.* **140**, 1669 (1995).
- [29] J. C. Bonner and M. E. Fisher, *Phys. Rev.* **135**, A640 (1964).
- [30] J. Glerup, P. A. Goodson, D. J. Hodgson and K. Michelsen, *Inorg. Chem.* **34**, 6255 (1995).
- [31] U. García-Couceiro, O. Castillo, A. Luque, G. Beobide and P. Román, *Inorg. Chim. Acta* **357**, 339 (2004).
- [32] D. J. Price, A. K. Powell and P. T. Wood, *J. Chem. Soc., Dalton Trans.*, 2478 (2003).